

# Optical waveguiding in suspensions of dielectric particles

Richard S. Conroy, Brian T. Mayers, Dmitri V. Vezenov, Daniel B. Wolfe, Mara G. Prentiss, and George M. Whitesides

An optical waveguide formed by a suspension of dielectric nanoparticles in a microchannel is described. The suspensions, chosen for their guiding and scattering properties, are silica and polystyrene particles that have diameters of 30–900 nm and are dispersed in water with volume fractions up to 10%. Changing the diameter and concentration of the particles causes the suspensions to transition from Rayleigh to Mie scattering and from single to multiple scattering. The threshold for optical guiding in a waveguide core composed of these suspensions is set by the numerical aperture of the effective refractive-index difference introduced by the suspension and not by the average interparticle distance. © 2005 Optical Society of America

OCIS codes: 290.5850, 230.7370.

An understanding of the transport of radiation in systems of disordered particles is important for many areas of science, from astronomy<sup>1</sup> to biological imaging.<sup>2</sup> The transmission function of these systems depends on the diameter, the distribution, and the composition of the particles. The optical properties of these systems, including the guiding and scattering of light in them, depends strongly on the wavelength of the radiation, the spatial distribution of the particles, and the magnitude and type of interparticle interactions. This dependence of the transmission characteristics on the properties of the particles has led to great interest in using dielectric spheres to create photonic bandgaps,<sup>3</sup> in random lasing,<sup>4</sup> and in Anderson localization.<sup>5</sup>

Previously it was shown that light can be generated,<sup>6</sup> guided, and manipulated<sup>7</sup> in laminar flows of liquids and solutions within microchannels, in circumstances in which the light was confined in a liquid core with a higher refractive index than that of the surrounding liquid cladding. This approach to forming liquid-core, liquid-cladding ( $L^2$ ) waveguides

is constrained by limitations on the ability to form and maintain refractive-index gradients and boundaries between different liquids. These gradients and boundaries between liquids are subject to diffusion, and the time over which they can be used is therefore limited. We describe a system that circumvents some of the limitations of homogeneous aqueous solutions by using suspensions of insoluble, dielectric particles dispersed in the core stream to increase its effective refractive index and to reduce the diffusion constant to maintain waveguide definition.

The scattering of light by suspensions of dielectric spheres in liquid media was described previously.<sup>8</sup> Subjects of particular interest have been the transition from Rayleigh to Mie scattering<sup>9</sup> and from an ensemble of independent scatters to one that exhibits multiple and coherent scattering.<sup>10</sup> In this paper we characterize both of these transitions, and the effective refractive index, of a range of suspensions; we are particularly interested in the properties of the suspensions that are required for guiding light. The question that we address is whether the numerical aperture created by the effective refractive index of the suspended particles sets the threshold for guiding or whether the refractive index is determined by the granularity of the refractive index.

The microfluidic device used for the research reported here is similar in a design to one that we previously reported for  $L^2$  waveguiding<sup>7</sup> (Fig. 1). We fabricated a channel, with dimensions  $0.1 \text{ mm} \times 0.5 \text{ mm} \times 5 \text{ mm}$  (height  $\times$  width  $\times$  length), by rep-

---

The authors are with Harvard University, Cambridge, Massachusetts 62138. R. S. Conroy (rconroy@fas.harvard.edu) and M. G. Prentiss are with the Department of Physics, and R. S. Conroy, B. T. Mayers, D. V. Vezenov, D. B. Wolfe, and G. M. Whitesides are with the Department of Chemistry and Chemical Biology.

Received 29 March 2005; accepted 21 July 2005.

0003-6935/05/367853-05\$15.00/0

© 2005 Optical Society of America

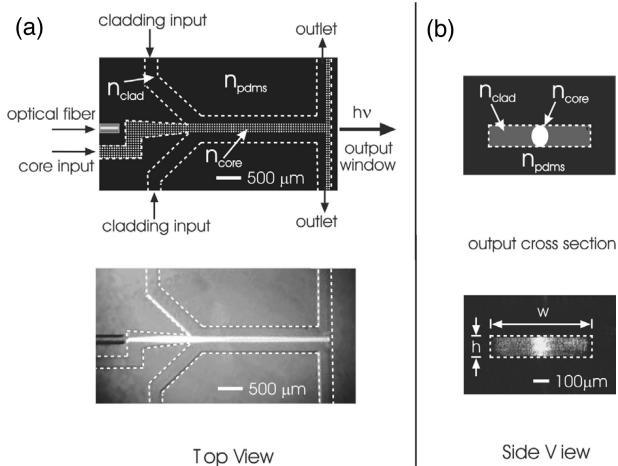


Fig. 1. Optical micrographs of the microfluidic device and operation with a core stream composition of 1% 50 nm polystyrene beads in water, and cladding streams of water. The edges of the channels are highlighted with dotted lines for clarity. (a) Top view, showing light scattered from the core stream. (b) End view at the exit window, showing light guided through the core against a background of scattered light.

lica molding of poly(dimethyl)siloxane (pdms;  $n = 1.406$ ), using rapid prototyping techniques.<sup>11</sup> The rates of flow of the core and cladding liquids were controlled with programmable syringe pumps (Kent Scientific). The core stream, containing a suspension of the dielectric particles in water, was brought within 100  $\mu\text{m}$  of the front facet of an optical fiber. This single-mode (N.A., 0.12) fiber carried light from a laser diode ( $\lambda = 635 \text{ nm}$ ). This light was used to characterize the guiding efficiency of the suspension. The core stream propagated away from the fiber and toward the output window. A waveguide was generated 1.5 mm from the fiber by the addition of a cladding stream composed of water ( $n = 1.331$ ) on either side of the core stream. After traveling 3.5 mm, the streams were diverted at right angles in front of the output windows in a T split to the two fluid outlets. Because the radius of curvature imposed on the liquid streams at the T split was small ( $\sim 250 \mu\text{m}$ ), light propagating in the core was decoupled and exited through an optically flat face of the pdms microchannel system. A  $10\times$  objective and a CCD camera were used to image the distribution of intensity of the guided light at the end of the channel. Figure 1 shows a micrograph of the output for a suspension of 50 nm diameter polystyrene beads (1% volume fraction in water and surfactant).

We focused our experiments on water-dispersed silica (Bangs Laboratories;  $n = 1.39$ ) and polystyrene (Bangs Laboratories, Duke Scientific, National Institute of Standards and Technology,  $n = 1.59$ ), with mean diameters  $a = 30\text{--}900 \text{ nm}$  and volume fractions in the core stream of as much as 10%. The particles formed a monodispersed suspension with a standard deviation from the mean of  $\leq 5\%$  in their diameter. The bulk optical properties of these suspensions were characterized with a spectrometer (HP

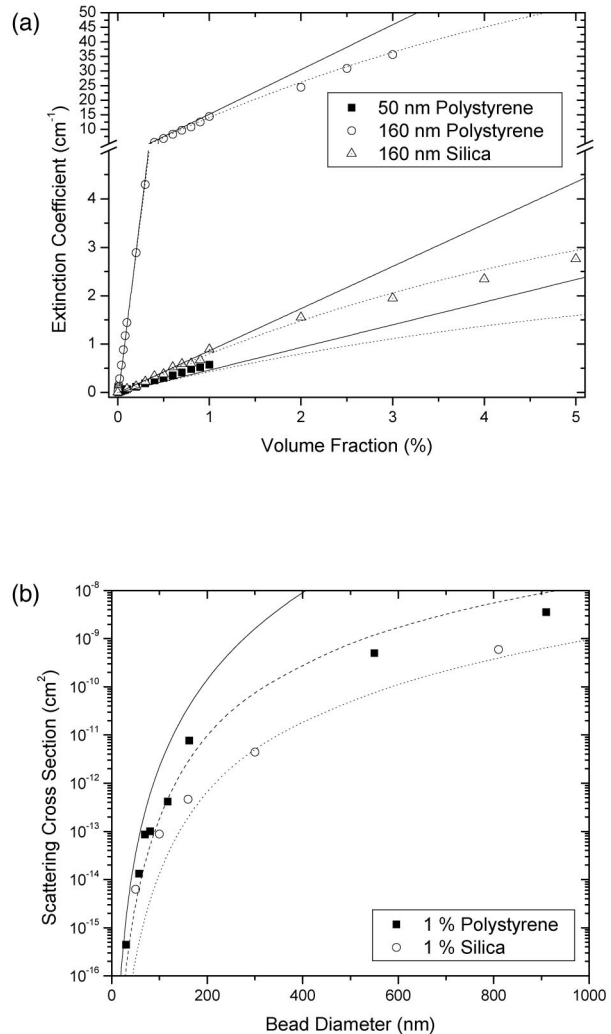


Fig. 2. (a) Measured extinction coefficient with expected values from independent (solid curves) and quasi-crystalline (dotted curves) scattering theory as a function of volume fraction for 50 and 162 nm polystyrene and 160 nm silica beads. (b) Measured scattering cross section of suspensions of particles of different diameters (1% volume fraction) with calculated values from Rayleigh (solid curve) and Mie (dashed curve, polystyrene; dotted curve, silica) scattering theory.

8453) using 1 cm and 1 mm path-length cuvettes and a refractometer (Bausch & Lomb Model 57).

Figure 2 summarizes the scattering properties of bulk suspensions of polystyrene and silica particles. Figure 2(a) is a plot of the extinction coefficient, measured with the spectrometer, as a function of increasing volume fraction for a selection of beads. At low volume fractions the turbidity increases linearly with volume fraction, consistent with the theory of independent scatters and Beer's law (solid curves). Above a volume fraction of 1% there is a small but significant deviation from this linear relationship for both silica and polystyrene; this deviation reflects significant multiple and coherent scattering. These results follow the trend predicted by the quasi-crystalline approximation theory,<sup>12</sup> which takes interparticle interactions into account and is represented by the dot-

ted curves in Fig. 2(a). The measured cross section deviates from Beer's law by more than 1% for volume fractions greater than 0.13%, this observation indicates that interactions are significant for interparticle spacing as much as ten times the diameter of a particle, in the range of diameters used for these experiments. Alternatively, if the effective scattering cross section from the turbidity data is plotted as a function of the diameter of the bead, then the scattering cross section is independent of volume fraction, with the 50 nm diameter polystyrene spheres [ $k(a/2) = (\pi n/\lambda)a = 0.33$ ] providing a good fit to the curve expected from Rayleigh scattering and the 0.16  $\mu\text{m}$  silica and polystyrene beads [ $k(a/2) = 1.05$ ] having a cross section between the calculated Rayleigh and Mie cross sections.

The effective refractive index of the bulk suspensions measured with the refractometer increased linearly with volume fraction, matching the value predicted by volume weighting. Comparison with the Maxwell-Garnett theory of mixing<sup>13</sup> indicates that there is only a small correction ( $\Delta n < -0.001$ ) for polystyrene with volume fractions up to 10%, although this correction becomes significant and measurable for mixtures with large refractive-index contrasts and reaches a maximum for volume fractions of 50–60%.

Figure 2(b) is a plot of measured scattering cross section versus bead diameter at a nominal volume fraction of 1% for the bulk suspensions. The solid and dotted curves correspond to the expected Rayleigh and Mie scattering cross sections, respectively. The transition from the Rayleigh [ $k(a/2) \ll 1$ ] to the Mie [ $k(a/2) > 1$ ] scattering regimes can be clearly seen for beads with diameter  $a = 50\text{--}200$  nm [ $k(a/2) = 0.33 - 1.3$ ]. The corresponding mean free paths are 2.5 cm for 50 nm polystyrene beads, 700  $\mu\text{m}$  for 160 nm polystyrene beads, and 1.4 cm for 160 nm silica beads, all at 1% volume fraction.

For a fixed volume fraction, the effective refractive index was independent of the diameter of the particles but dependent on their composition. The measured values for the silica beads matched the value predicted by volume weighting more closely ( $\pm 7\%$ ) than for the polystyrene beads ( $\pm 15\%$ ). We attribute the lower variability of the measured values for silica suspensions to the fact that all the silica particles came from a single manufacturer and remained in a stable suspension on storage and dilution.

We used the microfluidic system illustrated in Fig. 1 to test the ability of these suspensions of beads to guide light when we used them as the core stream in a  $L^2$  waveguide. We characterized the guiding efficiency as the ratio of the 635 nm traveling light intensity emitted at the end of core stream to that emitted from the cladding stream. The light in the cladding streams originates from small-angle scattering of light from the particles in the core. The relative intensities of light in the core and the cladding at the end of the channel therefore provide a measure of guiding efficiency versus scattering loss.

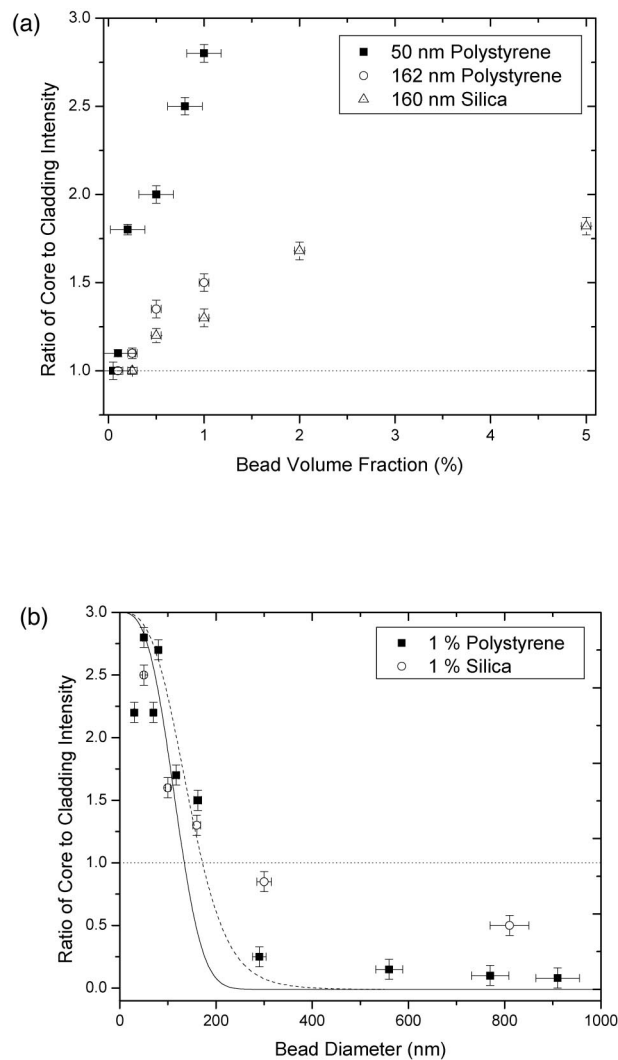


Fig. 3. Ratio of core to cladding intensity in the  $L^2$  waveguide as function of (a) volume fraction and (b) bead diameter. The solid (polystyrene) and dotted (silica) curves in (b) are the scaled transmission functions for an equivalent bulk sample. The horizontal dotted lines represent the intensity ratio observed in a homogeneous water core, water cladding system.

For maximizing guiding efficiency, the typical flow rates of  $\sim 1$  ml/h for the core and  $\sim 2$  ml/h for each of the cladding streams generated a roughly symmetric core cross section of approximate dimensions  $100 \mu\text{m} \times 100 \mu\text{m}$  [Fig. 1(B)]. Increasing or decreasing the aspect ratio reduced the intensity of the transmitted light. In wider core flows, the light intensity peaked at the interface between core and cladding streams because of the lower losses associated with these regions. For smaller core diameters, the effective refractive-index difference between core and cladding no longer supported waveguiding.

Owing to the laminar flow and to the relatively large diameter of the particles used here, the lateral diffusion of the particles during the time required for them to transit the channel (300 ms) was negligible. The transverse refractive-index profile can therefore

be considered a step function for the entire length of the waveguide.

Figure 3(a) shows the ratio of light intensity in the core to that in the cladding as a function of the volume fraction of beads suspended in the core, for those suspensions of beads that have three different diameters. As expected, the threshold volume fraction required for guiding increased with increasing bead diameter and decreased with increasing refractive index of the bead. For the 50 nm polystyrene beads the threshold volume fraction for guiding was 0.05%, corresponding to a refractive-index difference ( $n_{\text{core}} - n_{\text{clad}} = 1.3 \times 10^{-4}$ ). For comparison, the measurement was repeated with a homogeneous solution of styrene ( $n = 1.574$ ) in methanol ( $n = 1.329$ ) as the core and with pure methanol as the cladding. The threshold volume fraction in this case was 0.02%, and ( $n_{\text{core}} - n_{\text{clad}} = 4.9 \times 10^{-5}$ ), agreeing with the calculated refractive-index contrast required for propagation of a diffraction-limited mode in a waveguide with a core of 100  $\mu\text{m}$  diameter.

We can rationalize the relation between volume fraction ( $f \propto \Delta n$ ) and guiding efficiency, shown in Fig. 3(a), qualitatively. In the small-angle approximation the numerical aperture increases as the square root of the difference in refractive index between the core and cladding ( $\text{N.A.} \propto \sqrt{\Delta n}$ ). The effective solid capture angle is the square of the numerical aperture ( $\theta \propto \text{N.A.}^2 \propto \Delta n \propto f$ ); thus there is an approximately linear relationship between the volume fraction of particles in the core and the guiding efficiency of the core. As the volume fraction of beads increases, the numerical aperture of the fluid core approaches the numerical aperture of the input fiber (the numerical aperture of the fiber is 0.12, corresponding to volume fractions of  $f = 3\%$  for polystyrene and 15% for silica), and there is a decrease in guiding efficiency. With further increase of the volume fraction, the turbidity of the core continues to increase approximately linearly with the volume fraction of the particles, but there is no increase in the intensity of light that can be captured from the fiber; therefore overall guiding efficiency decreases. Thus the numerical aperture of the input light and the refractive index of the particles determine the volume fraction of suspended particles required for optimal guiding efficiency.

For the 160 nm diameter beads and light at 635 nm, the minimum volume fractions of particles required for guiding were 0.25% for polystyrene and 0.5% for silica. For the 160 nm polystyrene particles, this volume fraction corresponds to a particle density of  $1.1 \times 10^{12} \text{ cm}^{-3}$  and an interparticle distance of 1.0  $\mu\text{m}$ , or 2.1 times the wavelength of 635 nm light in water (477 nm). An average density of one particle per wavelength occurs for a volume fraction of 2% for 160 nm diameter particles. Thus the threshold for guiding is determined by the diameter and the numerical aperture of the core, defined by the effective refractive-index change caused by the presence of the suspension of particles. At low densities, when the

interparticle spacing is more than the wavelength of light, the granularity of the refractive index does not limit the guiding efficiency.

Figure 3(b) shows the ratio of the light intensity in the core to that in the cladding ( $I_{\text{core}}/I_{\text{clad}}$ ) as a function of bead diameter for a nominal volume fraction of 1%. Guiding is extinguished as the particle diameter and hence the turbidity increases, with a crossover particle diameter ( $\sim 225 \text{ nm}$ ) measurably larger than the transition predicted by theory between Rayleigh and Mie scattering [ $k(a/2) = 1$ ; diameter,  $\sim 150 \text{ nm}$ ]. Figure 3(b) also shows the transmission function, calculated from Rayleigh–Gans theory,<sup>8</sup> plotted for polystyrene (solid curve) and silica (dotted curve). The transition to antiguiding ( $I_{\text{core}}/I_{\text{clad}} < 1$ ) is sharper for polystyrene than for silica but has a similar critical particle diameter. Although the scattering cross sections for silica and polystyrene beads of the same diameter differ by a factor of 20, the numerical aperture of the silica beads is a factor of 5 less than that for polystyrene for the same volume fraction. This difference between the guiding efficiency as a function of bead diameter and the equivalent absorption data indicates that, in addition to photons that are not scattered, forward-scattered photons are also guided with higher efficiency for suspensions of polystyrene than suspensions of silica at the same volume fraction because of the larger refractive-index contrast between the core and cladding streams.

In classical waveguides, scattering losses are deleterious. Controlled scattering can, however, lead to the generation of optical bandgaps and random lasing. Heterogeneous suspensions of solid particles offer a number of advantages over homogeneous solutions of dyes for the  $L^2$  waveguides: (i) diffusion of the core is negligible, (ii) insoluble materials can be used, and (iii) particles with a core–shell or crystalline structure can be optically–electrically–magnetically manipulated. The primary disadvantages of using a suspension of solid particles in a liquid are that (i) there are increased scattering losses, (ii) high volume fractions are required for localization of the light field to be seen, and (iii) clogging can occur in channels. Combining the heterogeneous suspensions and homogeneous solutions of dyes makes these  $L^2$  waveguides particularly useful for exploring the phenomena of random lasing by providing two-dimensional confinement of the light in a reconfigurable geometry.

To our knowledge, these results are the first demonstration of waveguiding in a liquid core containing a suspension of scattering particles and the first analysis of the requirements for guiding in dilute, discrete systems. Our observation that guiding is limited not by the interparticle spacing but by the effective numerical aperture of the core containing the suspension is supported by recent results of examining light transport in cold atoms.<sup>14</sup> More generally, this system is attractive for studying light transport in scattering media because particle concentration is rapidly reconfigurable, from dilute, disordered streams to high-volume-fraction quasi-crystalline states.

This research was supported in part by a Defense Advanced Research Projects Agency subaward from the California Institute of Technology. The content of the information does not necessarily reflect the position or the policy of the U.S. government, and no official endorsement should be inferred.

## References

1. B. T. Draine, "interstellar dust grains," *Annu. Rev. Astron. Astrophys.* **41**, 241–289 (2003).
2. J. C. Hebden, S. R. Arridge, and D. T. Delpy, "Optical imaging in medicine. 1. Experimental techniques," *Phys. Med. Biol.* **42**, 825–840 (1997).
3. M. L. Povinelli, S. G. Johnson, E. Lidorikis, J. D. Joannopoulos, and M. Soljacic, "Effect of a photonic band gap on scattering from waveguide disorder," *Appl. Phys. Lett.* **84**, 3639–3641 (2004).
4. X. H. H. Wu, A. Yamilov, H. Noh, H. Cao, E. W. Seelig, and R. P. H. Chang, "Random lasing in closely packed resonant scatterers," *J. Opt. Soc. Am. B.* **21**, 159–167 (2004).
5. D. S. Wiersma, P. Bartolini, A. Lagendijk, and R. Righini, "Localization of light in a disordered medium," *Nature* **390**, 671–673 (1997).
6. D. V. Vezenov, B. T. Mayers, R. S. Conroy, G. M. Whitesides, P. T. Snee, Y. Chan, D. G. Nocera, and M. G. Bawendi, "A low-threshold, high-efficiency microfluidic waveguide laser," *J. Am. Chem. Soc.* **127**, 8952–8953 (2005).
7. D. B. Wolfe, R. S. Conroy, P. Garstecki, B. T. Mayers, M. A. Fischbach, K. E. Paul, M. Prentiss, and G. M. Whitesides, "Dynamic control of liquid-core/liquid-cladding optical waveguides," *Proc. Nat. Acad. Sci. USA* **101**, 12434–12438 (2004).
8. H. C. van der Hulst, *Light Scattering by Small Particles* (Dover, 1957).
9. A. J. Cox, A. J. DeWeerd, and J. Linden, "An experiment to measure Mie and Rayleigh total scattering cross sections," *Am. J. Phys.* **70**, 620–625 (2002).
10. A. Quirantes, F. Arroyo, and J. Quirantes-Ros, "Multiple light scattering by spherical particle systems and its dependence on concentration: a T-matrix study," *J. Coll. Interf. Sci.* **240**, 78–82 (2001).
11. J. C. McDonald and G. M. Whitesides, "Poly(dimethylsiloxane) as a material for fabricating microfluidic devices," *Acc. Chem. Res.* **35**, 491–499 (2002).
12. V. P. Dick, "Applicability limits of Beer's law for dispersion media with a high concentration of particles," *Appl. Opt.* **37**, 4998–5004 (1998).
13. J. C. M. Garnett, "Colours in metal glasses and in metallic films," *Phil. Trans. R. Soc. London* **203**, 385–420 (1904).
14. M. Vengalatorre, "Atom–light interactions in ultracold anisotropic media," Ph.D. dissertation (Massachusetts Institute of Technology, 2005).